

Dual frequency circularly polarised microstrip antenna

R. Shavit, Y. Israeli, L. Pazin and Y. Leviatan

Abstract: A dual frequency and dual circular polarisation multilayer microstrip antenna element for satellite communication is presented. The element is fed by a gap-coupled probe pin. The microstrip element exhibits a dual frequency band of operation for two orthogonal circular polarisations. A parametric study to optimise the element performance has been conducted. A prototype with dimensions that are based on the simulations has been built and tested. A good agreement between the measured and numerical results was found.

1 Introduction

Microstrip patch antenna elements are very popular in wireless communication system applications. They offer an attractive way to integrate the RF front end of the system with its antenna and achieve a low profile, low weight, easy to fabricate and low cost solution. The increased demand for higher transmission capacity is driving the research to investigate new ways to increase the microstrip antenna bandwidth or, alternatively, operate in multiple frequencies while using two orthogonal polarisations. This requirement motivated our research to look for a dual frequency and dual circular polarisation antenna element for Ku band satellite communications. There are numerous ways to obtain a dual-band circularly polarised printed antenna as described in [1–4]. However, in all the above cases the same sense circular polarisation, right-hand circular polarisation (RHCP) or left-hand circular polarisation (LHCP), was investigated.

In this paper, a dual frequency and dual circular polarisation microstrip element is presented. The linear polarised, dual-frequency stacked circular antenna described in [5] inspired to some degree the proposed element. The element is composed of two stacked circular patches fed in tandem by a single gap-coupled probe pin [6]. The proposed element design is unique in the sense that it enables one to adjust independently the phase of the radiated electric field of each of the patches by turning each patch around its common feeding point. This is an important feature for the design of a microstrip non-resonant antenna array fed by a radial waveguide [7]. It enables one to adjust the phase so as to offset the phase errors generated in a radial waveguide microstrip array. The proposed element has been studied numerically and later built and tested. The computation of the antenna parameters and currents has been conducted using the

Microwave Studio (MWS) commercial software from Computer Simulation Technology (CST), which is based on the method of finite integral time domain (FITD) algorithm. A prototype of the element in Ku band has been built and tested. The agreement between the computed and the experimental results was good.

2 The element design

The basic structure of the proposed element operating in two Ku frequency bands and two orthogonal circular polarisations is shown in Fig. 1. Two stacked circular patches are fed in tandem by a single pin. Each patch is coupled to the feeding pin through an annular gap. This unique type of feeding is necessary in order to introduce a capacitive effect to counterbalance the inductive effect of the feeding pin. The feeding pin is top loaded with a little circular pad as an additional matching element. The upper patch ‘ground plane’ is the lower patch. To ensure a large enough ‘ground plane’ for the upper patch in all of its turning angular positions, the diameter of the upper patch (operating in the upper frequency band) must be considerably less than that of the lower patch (operating in the lower frequency band). This may be achieved by choosing the relative permittivity ϵ_r of the substrate between the lower patch and the ground plane to be close to unity, and on contrary by choice of considerably greater relative permittivity of the substrate between the two patches.

In the design of the proposed element the lowest layer is Rohacell foam with electrical properties $\epsilon_r = 1.067$, $\tan\delta = 0.0041$ and thickness 0.761 mm. The substrate between the two patches is Rogers RO4003 with electrical properties $\epsilon_r = 3.38$, $\tan\delta = 0.002$ and thickness 0.5 mm. The top pad is printed on the Rogers substrate RO4350 with electrical properties $\epsilon_r = 3.48$, $\tan\delta = 0.001$ and thickness 0.1 mm. A parametric study to optimise the element performances was conducted using MWS software from CST. For the operating frequencies 11.95 GHz (RHCP, lower patch) and 14.25 GHz (LHCP, upper patch), the patch diameters found are 11 mm and 5.85 mm, respectively, and the diameters of the annular gaps are 0.9 mm (inner) and 1.5 mm (outer). In a microstrip non-resonant antenna array fed by a radial waveguide configuration the top patch rotation angle varies from ring to ring and correspondingly its dimensions may change. The eccentricity of the annular gaps is chosen as 1.8 mm for the lower

© IEE, 2005

IEE Proceedings online no. 20045137

doi:10.1049/ip-map:20045137

Paper first received 24th October 2004 and in revised form 6th February 2005

R. Shavit and Y. Israeli are with the Department of Electrical and Computer Engineering, Ben-Gurion University of the Negev, Beer Sheva 84105, Israel

L. Pazin and Y. Leviatan are with the Department of Electrical Engineering, Technion, Haifa 32000, Israel

E-mail: rshavit@ee.bgu.ac.il

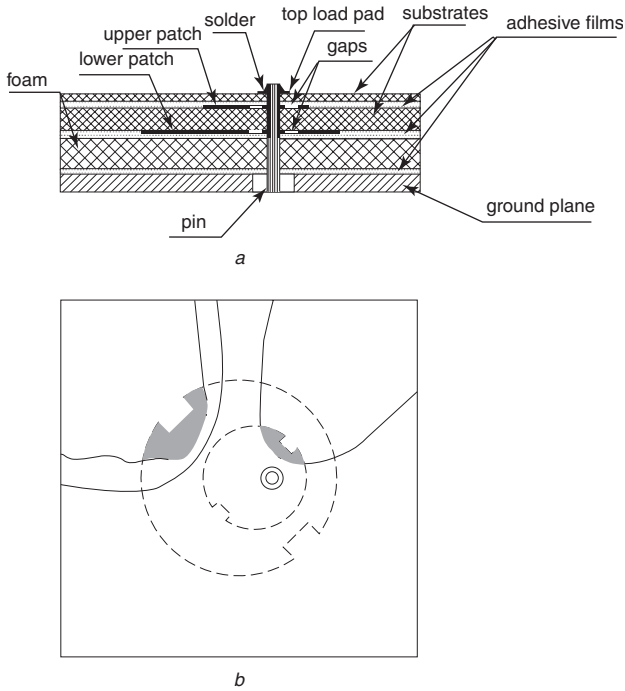


Fig. 1 Geometry of the dual frequency, dual circular polarisation microstrip antenna

a Cross-section

b Top view

patch and 0.9 mm for the upper patch, to match the radiation element 50 ohm input impedance [8]. The corresponding optimum pad diameter is 1.3 mm. The diameter of the feeding pin is equal to 0.3 mm and the diameter of the pin together with the soldered metalised layer in the substrate package is equal to 0.7 mm. The entire multilayer structure is bonded with adhesive films. The choice of the films has been made based on practical considerations and available adhesive films with electrical properties as close as possible to the corresponding substrate. The adhesive film used to bond the RO4350 substrate to the RO4003 substrate is of thickness 0.1 mm and electrical properties $\epsilon_r = 3.17$, $\tan\delta = 0.005$, while on both sides of the foam the adhesive films used are of thickness 0.03 mm and electrical properties $\epsilon_r = 5$, $\tan\delta = 0.005$. The circular polarisation is achieved for each circular patch by introducing two indents as described in [9]. The indent dimensions are 1.01×0.52 mm for the upper patch and 1.95×0.98 mm for the lower patch.

3 Numerical and test results

The antenna performance has been tested on a prototype element printed on a finite ground plane 4×4 cm. Figures 2 and 3 show the computed current distribution at the centre frequencies 11.9 GHz and 14.25 GHz on both patches. One can observe, that at 11.9 GHz only the lower patch is excited, while at 14.25 GHz the upper patch is excited emphasising, as expected that the two patches operate independently in the two frequency bands.

A thorough parameter investigation has been conducted to determine the sensitivity of the element performance to changes of various parameters like: foam thickness and substrate thicknesses. Figure 4 shows the effect of the foam thickness variation ($\pm 10\%$) on the return loss (RL). One can observe that this variation affects mainly the centre frequency in the lower band. Figure 5 shows the effect of the RO4003 substrate thickness variation ($\pm 10\%$) on the RL. In this case the variation in the substrate thickness affects mainly the centre frequency of the upper band. This observation indicates that the two patches operate almost independently with the foam variation affecting the lower patch operation and the RO4003 substrate variation affecting the upper patch performance. Figure 6 shows the effect of the RO4350 substrate thickness variation ($\pm 50\%$) on the RL. In this case the substrate variation affects both the lower and upper patch performances.

Preliminary inspection of the RL measurement results compared to the simulation results have indicated a slight shift in the centre frequency of the upper patch frequency band to 14 GHz and a more significant shift in the centre frequency of the lower patch frequency band to 11 GHz. At this point it was decided to verify the cross-section dimensions of the multilayer structure by bisecting the model and inspecting its dimensions with a microscope. The inspection revealed that some of the adhesive particles penetrated into the foam. Accordingly, the model has been revised and simulations repeated. Figure 7 shows a comparison between the measured and computed RL results of the prototype (original and revised models). In the revised simulation it has been assumed that the adhesive film thickness on both sides of the foam is 0.08 mm (compared to 0.03 mm used in the initial simulations), in accordance with the microscope dimensions findings. The revised simulation results are in a very good agreement with the measured data. The revised model geometry has been used to compute the radiation characteristics of the antenna element and compared to the measured data. Figure 8 shows a comparison between measured and simulated data

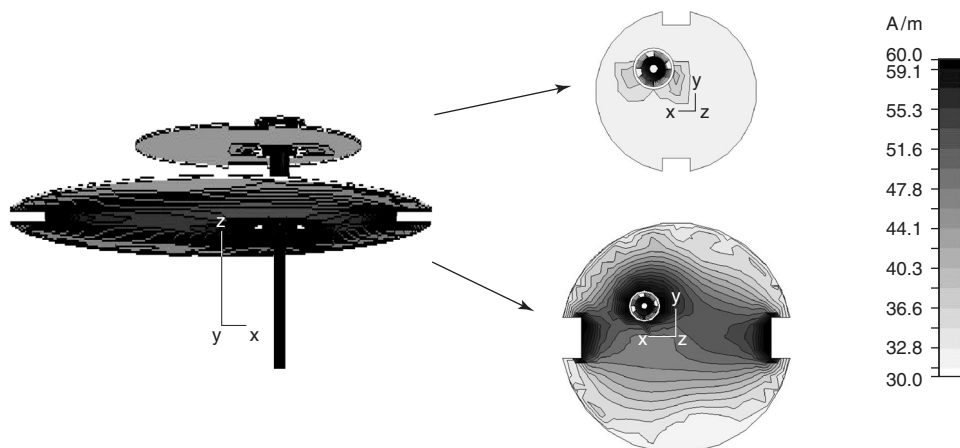


Fig. 2 Current distribution on patches at 11.9 GHz

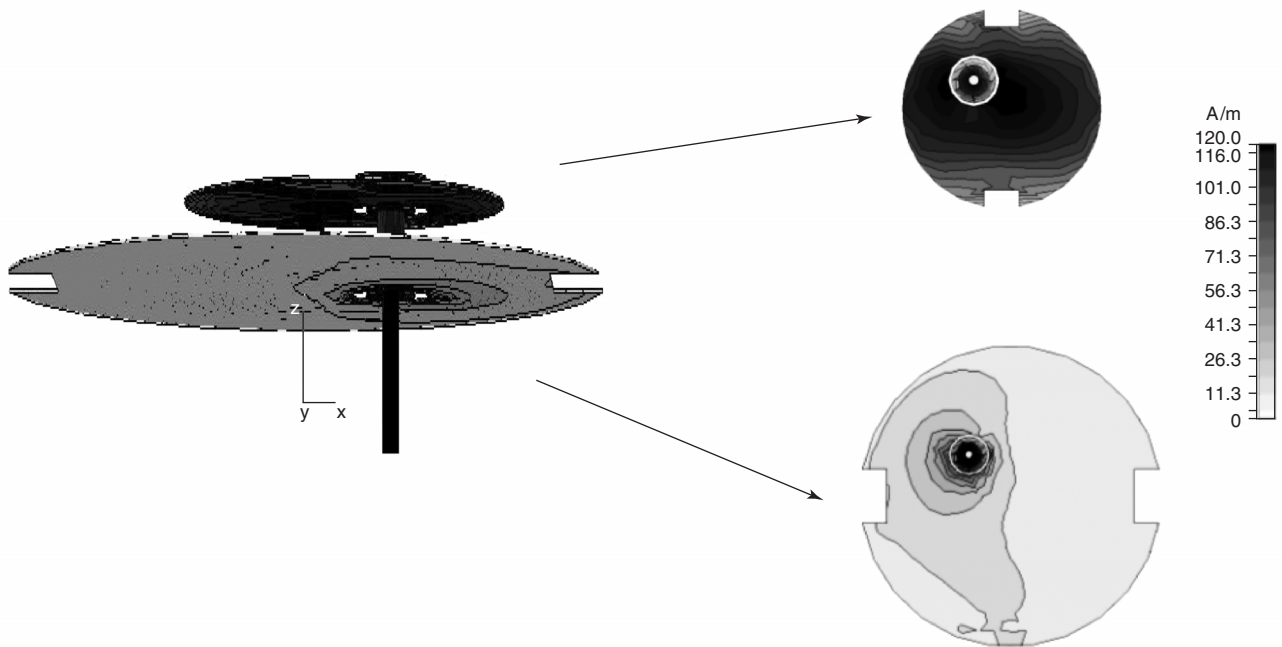


Fig. 3 Current distribution on patches at 14.25 GHz

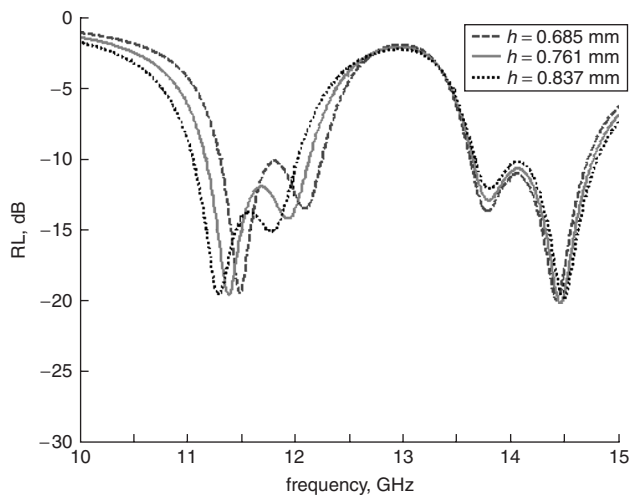


Fig. 4 Effect of foam thickness variation ($\pm 10\%$) on the RL

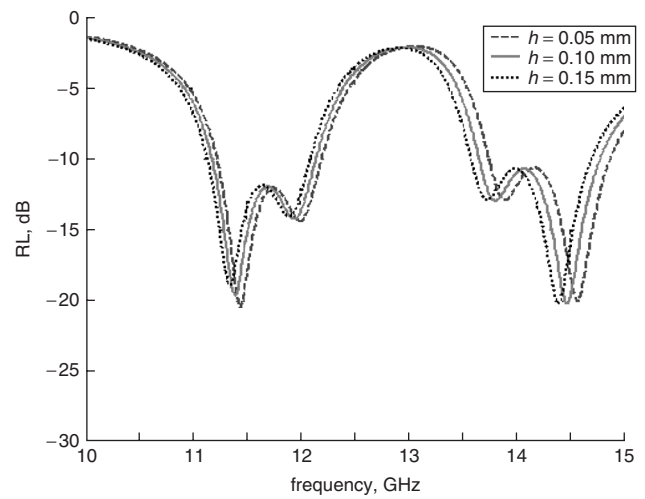


Fig. 6 Effect of RO4350 substrate thickness variation ($\pm 50\%$) on the RL

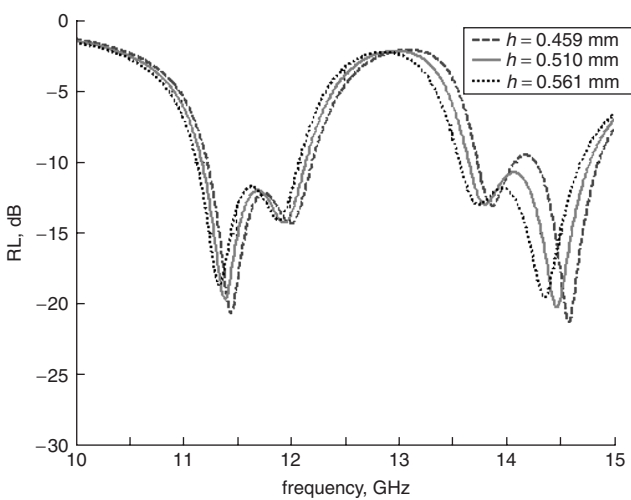


Fig. 5 Effect of RO4003 substrate thickness variation ($\pm 10\%$) on the RL

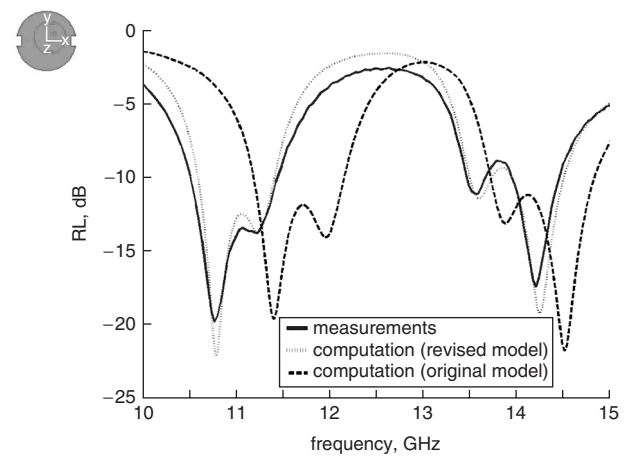


Fig. 7 Measured and computed data of the RL (on initial and revised models)

of the copol element gain (RHCP in the lower frequency band and LHCP in the upper frequency band). The circular copol gain has been measured by the phase-amplitude polarisation measurement method [10], in which a linear gain antenna has been used on the transmit side and the antenna under test (AUT) on the receive side to measure the complex amplitude for two orthogonal (vertical and horizontal) orientations of the AUT. The data recorded has been used to compute the field of the copol circular polarisation and compared to the received field by a standard linear gain antenna to obtain the circular copol gain. The maximum gain in the lower frequency band is 8 dBic, while in the upper frequency band is 4.3 dBic. The agreement between measured and simulated data is good. The variation in the gain of the element in the upper and lower frequency bands can be traced to the fact that the upper patch is printed on a substrate with a higher dielectric constant than that of the lower patch. This difference in

the substrate electrical properties affects the gain of the radiating patches, since the gain is inversely proportional to the dielectric constant of the patch substrate [11]. Figure 9 shows a comparison between measured and simulated data of the element axial ratio (AR) as a function of frequency in both frequency bands. The AR on the boresight axis of the element is 1 dB, while the 3 dB bandwidth is 2% in the lower frequency band and 1.5% in the upper frequency band. The agreement between measured and simulated data is good. The AR at the centre frequencies is not better than 1 dB, owing to excitation of two imbalanced orthogonal modes in the patch by the gap coupled finite diameter feeding pin. This imbalance is also manifested in the RL plot as shown in Fig. 7. Figure 10 shows a comparison between measured and simulated data of the element's copol radiation patterns in elevation ($x-z$ plane) for the new centre frequencies (11 GHz in the lower frequency band and 14 GHz in the upper frequency band)

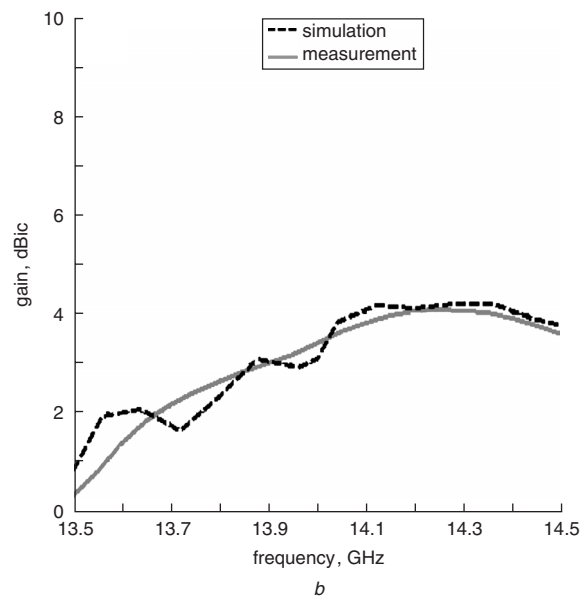
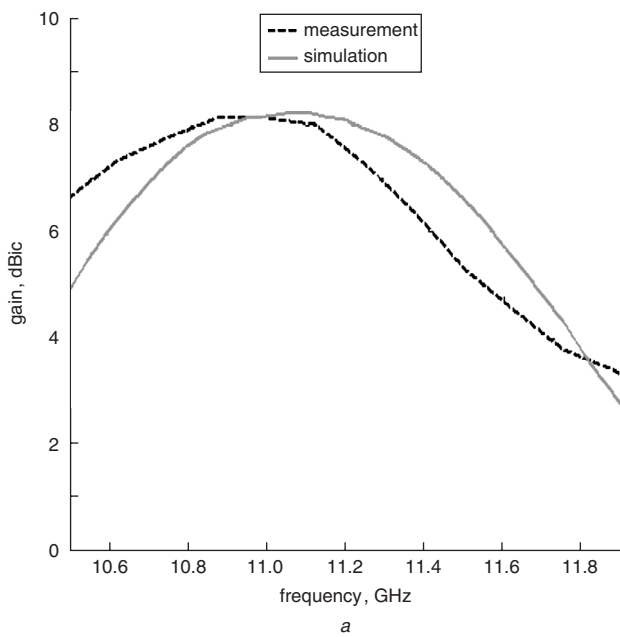


Fig. 8 Gain against frequency (measured and computed) of the microstrip element
a Low frequency band
b High frequency band

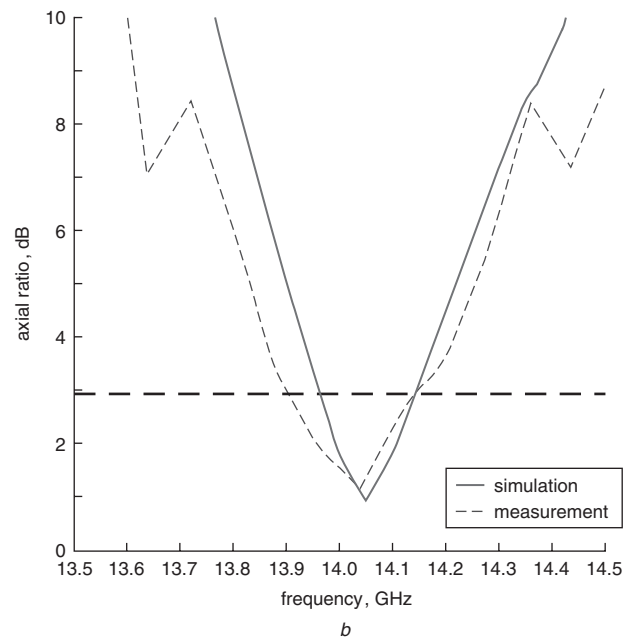
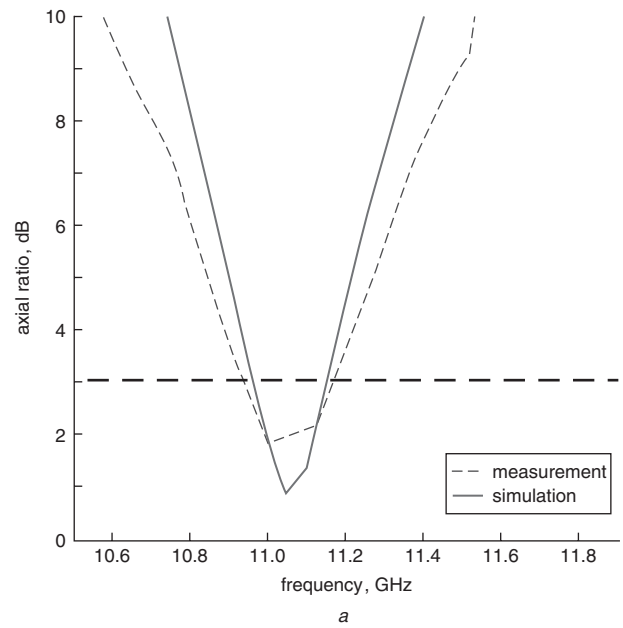


Fig. 9 Axial ratio against frequency (measured and computed)
a Low frequency band
b High frequency band

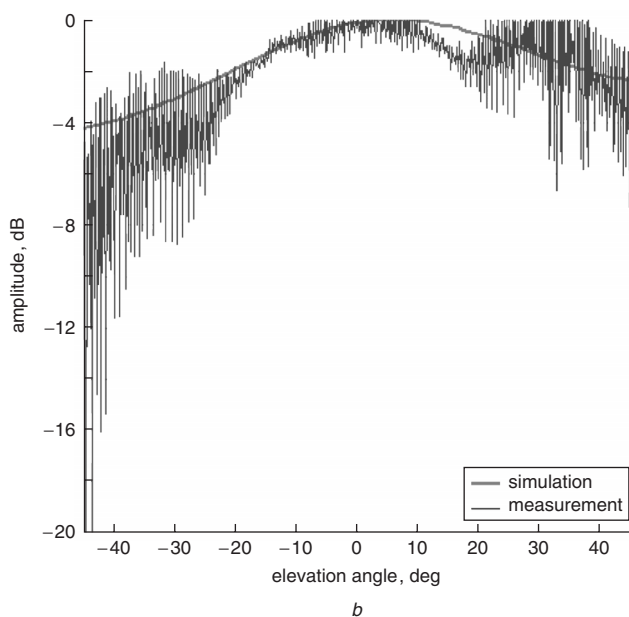
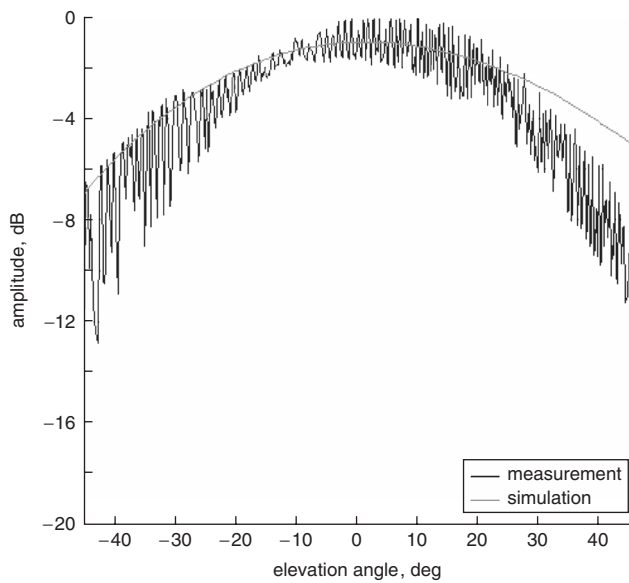


Fig. 10 Radiation patterns in x - z plane of the microstrip element
a At 11 GHz
b At 14 GHz

of the fabricated model. The measured data has been acquired with the AUT being at the receiving end and with a linear polarisation horn rotated around its axis being at the transmitting end. The simulated data describe the RHCP and LHCP copol radiation patterns for the lower and upper frequency bands, respectively. One can observe that the average amplitude of the receiving signal follows closely the simulated copol (RHCP or LHCP) data in both frequency bands. The 3 dB beamwidth is approximately 60° in both frequency bands. Moreover, one can notice an asymmetry in the radiation pattern at 14 GHz with respect to the boresight direction. This degradation in the CP radiation pattern can be explained by the fact that the upper patch is not centred above the lower patch, which serves as its ground plane.

To investigate the dependence of the radiated electrical phase variation with the upper patch rotation, three more prototypes with the upper patch turned around the feeding point (lower patch remaining fixed) at 30° , 60° and 90° have

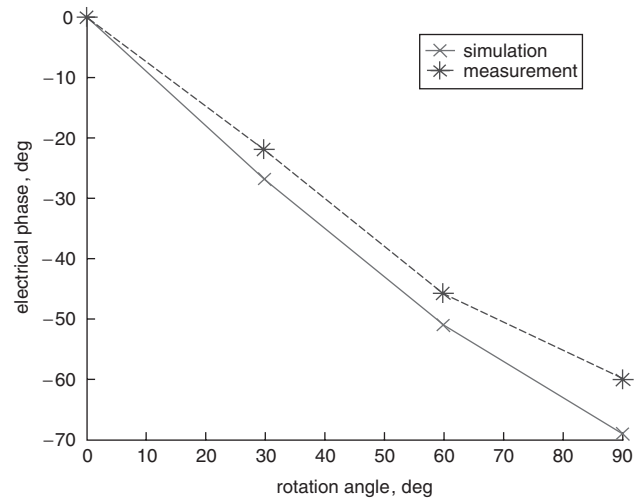


Fig. 11 Electrical phase dependence on the rotation angle of the upper patch at 14 GHz

been fabricated and measured. The dependence of the radiated electrical phase at 11 GHz on the rotation angle of the lower patch around the feeding point has been tested and found to be linear as expected. In contrast, the dependence of the radiated electrical phase at 14 GHz (the centre frequency in the revised model), on the rotation angle of the upper patch with the lower patch fixed is not linear as shown in Fig. 11. In a perfect scenario it is expected that the dependence should be linear, however owing due to the inherent asymmetric nature of the structure (the upper patch vis-à-vis the lower patch) a nonlinear dependence was obtained. This nonlinearity may be easily taken into account by determination of the upper patch positions during the designing procedure of the radiating antenna element for a multi-ring circular array. To reduce the nonlinearity of the phase dependence a possible way is to increase the dielectric constant of the substrate on which the upper patch is printed. Such a move will reduce the diameter of the upper patch such that throughout its turning it will encounter a more uniform ground plane exhibited by the lower patch.

4 Conclusions

A dual frequency and dual circular polarisation multilayer microstrip antenna element fed by a gap-coupled probe pin has been presented. The microstrip element exhibits a satisfactory performance in two Ku frequency bands. Fabrication accuracy problems in the dimensions of the original layers structure caused a discrepancy between the measured and simulations results of the original design. Simulations of the revised model based on the actual prototype dimensions have been performed and a good agreement with the measurement results was found. The dependence of the radiated electrical phase (lower Ku band) on the lower patch turning has been found to be linear, while the dependence of the radiated electrical phase (upper Ku band) on the upper patch turning with the lower patch fixed has been found to be quasi-linear.

5 Acknowledgments

The authors wish to thank M. Sigalov, for performing the measurements on the manufactured prototypes. This

project was supported by ISIS consortium, Trade and Industry Ministry, Israel.

6 References

- 1 Pozar, D.M., and Duffy, S.M.: 'A dual-band circularly polarized aperture-coupled stacked microstrip antenna for global positioning satellite', *IEEE Trans. Antennas Propag.*, 1997, **45**, pp. 1618–1625
- 2 Su, C.M., and Wong, K.L.: 'A dual-band GPS microstrip antenna', *Microw. Opt. Technol. Lett.*, 2002, **33**, pp. 238–240
- 3 Jan, J.Y., and Wong, K.L.: 'A dual-band circularly polarized stacked elliptic microstrip antenna', *Microw. Opt. Technol. Lett.*, 2000, **24**, pp. 354–357
- 4 Balakrishnan, B., and Kumar, G.: 'Dual band circularly polarized off-centered EMCP antennas'. IEEE AP-S Int. Symp. Digest, 1998, pp. 316–319
- 5 Long, S.A., and Walton, M.D.: 'A dual-frequency stacked circular-disc antenna', *IEEE Trans. Antennas Propag.*, 1979, **AP-27**, pp. 270–273
- 6 Hall, P.S.: 'Probe compensation in thick microstrip patches', *Electron. Lett.*, 1987, **23**, pp. 606–607
- 7 Pazin, L., and Leviatan, Y.: 'Effect of amplitude tapering and frequency-dependent phase errors on radiation characteristics of radial waveguide fed non-resonant array antenna', *IEE Proc., Microw. Antennas Propag.*, 2004, **151**, pp. 363–369
- 8 Long, S.A., Shen, L.C., Walton, M.D., and Allerdig, M.R.: 'Impedance of a circular-disc printed circuit antenna', *Electron. Lett.*, 1978, **14**, pp. 684–686
- 9 Haneishi, M., Nambara, T., and Yoshida, S.: 'Study on elliptical properties of singly-fed circularly polarised microstrip antennas', *Electron. Lett.*, 1982, **18**, pp. 191–193
- 10 Antenna Standards Committee: 'IEEE Standard test procedures for antennas', ANSI/IEEE Std 149-1979, 1980, pp. 61–78
- 11 Long, S.A., Shen, L.C., and Morel, P.B.: 'Theory of the circular-disc printed circuit antenna', *Proc. Inst. Electr. Eng.*, 1978, **125**, pp. 925–928